Aerosol Science and Technology

ISSN: (Print) (Online) Journal homepage: www.tandfonline.com/journals/uast20

Evaluating source control efficacy against exhaled submicron particles: Total outward leakage of surgical masks and half facepiece respirators across a spectrum of particle sizes

Weihua Yang, Warren R. Myers, Mike Bergman, Edward Fisher, Kenneth J. Ryan, Brooke Vollmer, Lee Portnoff & Ziqing Zhuang

To cite this article: Weihua Yang, Warren R. Myers, Mike Bergman, Edward Fisher, Kenneth J. Ryan, Brooke Vollmer, Lee Portnoff & Ziqing Zhuang (2025) Evaluating source control efficacy against exhaled submicron particles: Total outward leakage of surgical masks and half facepiece respirators across a spectrum of particle sizes, Aerosol Science and Technology, 59:4, 487-498, DOI: 10.1080/02786826.2024.2427282

To link to this article: https://doi.org/10.1080/02786826.2024.2427282

Published online: 25 Nov 2024.

AEROSOL SCIENCE AND TECHNOLOGY
2025, VOL. 59, NO. 4, 487–498
https://doi.org/10.1080/02786826.2024.2427282

Evaluating source control efficacy against exhaled submicron particles: Total outward leakage of surgical masks and half facepiece respirators across a spectrum of particle sizes

Weihua Yang[a,b], Warren R. Myers[a], Mike Bergman[b], Edward Fisher[b], Kenneth J. Ryan[c], Brooke Vollmer[b], Lee Portnoff[b], and Ziqing Zhuang[b]

[a]Department of Industrial and Management Systems Engineering, West Virginia University, Morgantown, West Virginia, USA; [b]Centers for Disease Control and Prevention, National Institute for Occupational Safety and Health, National Personal Protective Technology Laboratory, Pittsburgh, Pennsylvania, USA; [c]Department of Statistics, West Virginia University, Morgantown, West Virginia, USA

ABSTRACT

The size of airborne particles emitted from infected individuals is crucial in the transmission of respiratory viruses. The use of source control devices is essential for interrupting the transmission of exhaled submicron particles, particularly in healthcare settings with high infection risk. This study evaluated the efficacy of five types of source control devices, commonly used in healthcare settings, in mitigating the transmission of exhaled submicron particles (20–210 nm). Total outward leakage (TOL) of these devices was analyzed across different particle sizes, and the TOL mean diameter (TOLMD) was calculated to characterize particle size distribution. The devices tested included N95 filtering facepiece respirators (N95 FFRs), N95 FFRs with an exhalation valve (N95 FFRV), surgical masks (SMs), elastomeric half-mask respirators (EHMRs), and EHMRs with a SM covering the exhalation valve (EHMRSM). The study also examined the effects of faceseal and flowrate on TOL and particle size characteristics. Results indicated that TOL varied with particle size, increasing from 40 to 90 nm before stabilizing. Aerosols larger than 90 nm had significantly higher TOL compared to smaller aerosols. Higher flow rates increased TOL for EHMR and EHMRSM across all particle sizes. Improved faceseal on N95 FFRs and SMs significantly reduced TOL and decreased TOLMD. The study underscored that using well-fitting devices without exhalation valves is crucial for preventing the transmission of exhaled aerosols potentially carrying viruses, in particular for larger particle sizes. This is especially crucial in the absence of proper indoor ventilation and other control measures.

ARTICLE HISTORY
Received 23 July 2024
Accepted 8 October 2024

EDITOR
Kihong Park

GRAPHICAL ABSTRACT

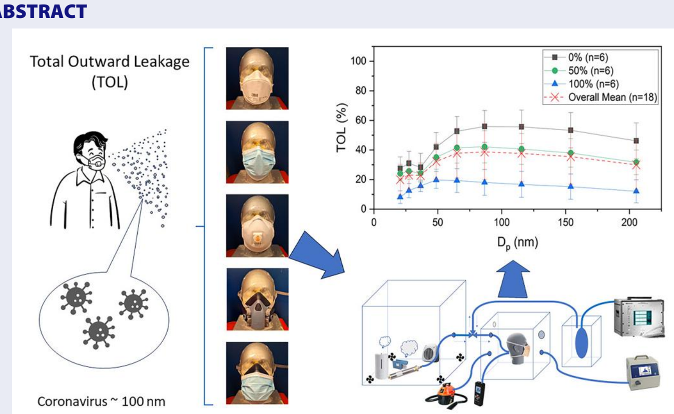

Introduction

Human respiratory activities, including breathing, talking, coughing, and sneezing, generate aerosols with multimodal size distributions ranging from 0.1 to 1000 μm (Pöhlker et al. 2021; Chatterjee et al. 2021; Prather, Wang, and Schooley 2020). These aerosols generated by human respiratory activities serve as carriers of infectious viruses, such as SARS-CoV-2 and

CONTACT Ziqing Zhuang zaz3@cdc.gov 626 Cochrans Mill Road, Pittsburgh, PA 15236, USA

influenza. Researchers detected influenza in aerosols smaller than 5 μm, with a significant fraction of particles measuring less than 1 μm (Fennelly 2020). Considerable evidence suggests that SARS-CoV-2 virions primarily travel in particles ranging from $\sim$0.1 to $\sim$10 μm (Pöhlker et al. 2021).

The aerosols carrying viruses have been demonstrated to spread through air and contact (World Health Organization 2024; Wang et al. 2021). Transmission through air is a particularly concerning route of transmission for respiratory viruses (World Health Organization 2024). Studies have demonstrated that SARS-CoV-2 and influenza typically spread through airborne transmission (Pöhlker et al. 2021; Samet et al. 2021; Wang et al. 2021; Prather et al. 2020).

To prevent the spread of airborne virus-laden particles, a well-fitted face mask or a respirator approved by the National Institute for Occupational Safety and Health (NIOSH), such as an N95® filtering facepiece respirator (N95 FFR), has been recommended to be worn by an infectious patient for source control to prevent further spread of disease (CDC 2022; Cheng et al. 2021; Fennelly 2020). The term "source control" refers to the measures taken to limit the transmission of disease by reducing the exhaled emissions of an infected individual into the environment (ASTM 2020). Respirators can also protect the wearer from inhaling airborne particles that may contain infectious organisms.

When an infected patient or healthcare personnel uses a respirator or face mask as a source control product, the outward leakage from the device during exhalation can contaminate the surrounding air, increasing the risk of aerosol exposure to others (Grinshpun and Yermakov 2021). Studies on the outward leakage of various respirators and face masks showed that these protective devices could not entirely isolate aerosol emissions from their source (Lindsley et al. 2021a, 2021b; Portnoff et al. 2021). Myers et al. (2023) defined and quantified total outward leakage (TOL) as a metric of the evaluation for source control efficacy. The TOL refers to all the outward leakage through and around a respirator or face mask. It is comprised outward penetration through the filter material, the leakage through the faceseal of the device, and the aerosol jet through the exhalation valve if one is present.

The ability of surgical masks (SMs) to interrupt transmission through air depends on particle size (Bourouiba 2021; Mittal, Ni, and Seo 2020; Prather, Wang, and Schooley 2020). The use of an SM, a type of loose-fitting face mask cleared by the U.S. Food and Drug Administration, has been recommended for preventing interpersonal infections based on the premise that most infectious particles travel in large respiratory droplets (>5 μm) (Fennelly 2020). Pöhlker et al. (2021) reported that SMs had higher collection efficacies for particles >5 μm, while their efficacy for collecting particles <5 μm was significantly lower (Pöhlker et al. 2021). Milton et al. (2013) determined that SMs reduced the influenza viral copies carried by aerosols $\leq$5 μm by 2.8 times, while for aerosols >5 μm the SMs reduced the influenza viral copies by 25 times (Milton et al. 2013). The lowest filtration efficiency of SMs was reported to be 30.5% at around 250 nm (Rengasamy, Eimer, and Shaffer 2010). Additionally, the study found that the faceseal gap significantly decreased the protective efficiency of SMs against particles >100 nm (Konda et al. 2020).

Because N95 filtering facepiece respirators (N95 FFRs) were not originally designed to be used as source control devices, most studies have focused on inhalation penetration, which is also dependent on particle size. Many studies have revealed that N95 FFRs have better filtration efficiency against particles greater than $\sim$300 nm than those smaller than $\sim$300 nm (Joshi, Khan, and Sapra 2022; Konda et al. 2020, 2020; Lu et al. 2020). Other studies have shown that the most penetrating particle size (MPPS) of N95 FFRs against charge-neutralized NaCl aerosols was in a range of 0.03–0.3 μm (Shaffer and Rengasamy 2009; Lee, Grinshpun, and Reponen 2008; Balazy et al. 2006; Qian et al. 1998). A recent study by Duncan, Bodurtha, and Naqvi (2021) reported that 0.076 μm particles had the highest inhalation penetration of 3.41% across all the N95 FFR models evaluated (Duncan, Bodurtha, and Naqvi 2021).

Although researchers have made observations made on the outward leakage through the exhalation valve of N95 FFRs equipped with an exhalation valve (N95 FFRVs) using visualization technology (Staymates 2020; Verma, Dhanak, and Frankenfield 2020), limited studies exist on N95 FFRV TOL that consider particle size. A recent study investigating the barrier performance of various respiratory protective devices in preventing bacterial contamination of the sterile field suggested that 10% of the exhaled bioaerosol falls below $\sim$1.6 μm when using an EHMR with an exhalation valve (Myers et al. 2022). However, this evidence is insufficient to infer the efficacy of EHMRs in mitigating the spread of smaller particles carrying viruses when used for source control.

An evaluation of TOL as a function of particle size would provide useful insight on the ability for respirators and face masks to provide source control and may help to elucidate how exhaled aerosols emitted through respirators and face masks travel in the ambient air. In contrast to our previous study (Myers et al. 2023), which reported only the overall TOL of these devices without accounting for particle size variation, our thist study offers a more comprehensive analysis by evaluating the TOL of five different devices—SM, NIOSH Approved® N95 FFRs, N95 FFRVs, EHMRs, and EHMRs with a SM covering the exhalation valve (EHMRSMs)—specifically for submicron particles ranging from 20 to 210 nm. This study introduced a new dimension by investigating the relationship between TOL and particle size, offering a more detailed understanding of how these devices perform across different particle sizes. Additionally, this work assesses the impact of varying faceseal conditions on TOL, with three artificially created faceseal levels, and examined how different flowrates generated by a breathing simulator affect TOL across particle sizes. These elements, not explored in the previous study, highlighted the novel contributions of this work in understanding the performance of respiratory protective devices for source control.

Methods

Table 1 lists the information on the devices tested. The experimental setup for the TOL across particle sizes collection system in this study, as shown in Figure 1, was identical to that described in detail in our previous study (Myers et al. 2023). In this study, we generated aerosols under controlled conditions in a large chamber where temperature and relative humidity were maintained at 32 ± 2 °C and 60 ± 2%, respectively. To simulate human breathing, we utilized a breathing simulator (Model 1101; Hans Rudolph, Inc., Shawnee, KS, USA) with a cyclical breathing model.

We fitted the tested devices onto a hard-surface headform, which we then placed within the small chamber. The generated aerosols were subsequently directed toward the headform in this setup. We

Table 1. Information on the devices tested (Myers et al. 2023).

Type	Manufacturer	Model	Picture	Manufacturer	Model	Picture
SM	Cardinal Health	–		Aleen	–	
N95 FFR	3M TC-84A-8590	Aura9205	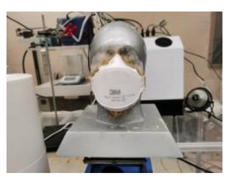	Fangtian TC-84A-7863	N058	
N95 FFRV	3M TC-84A-5669	Aura9211		3M TC-84A-1299	8511	
EHMR	MSA TC-84A-6764	200LS		3M TC-84A-0022	7503	
EHMRSM	MSA+ Cardinal Health	200LS		3M + Cardinal Health	7503	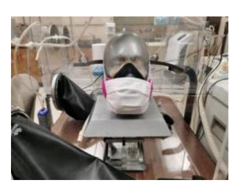

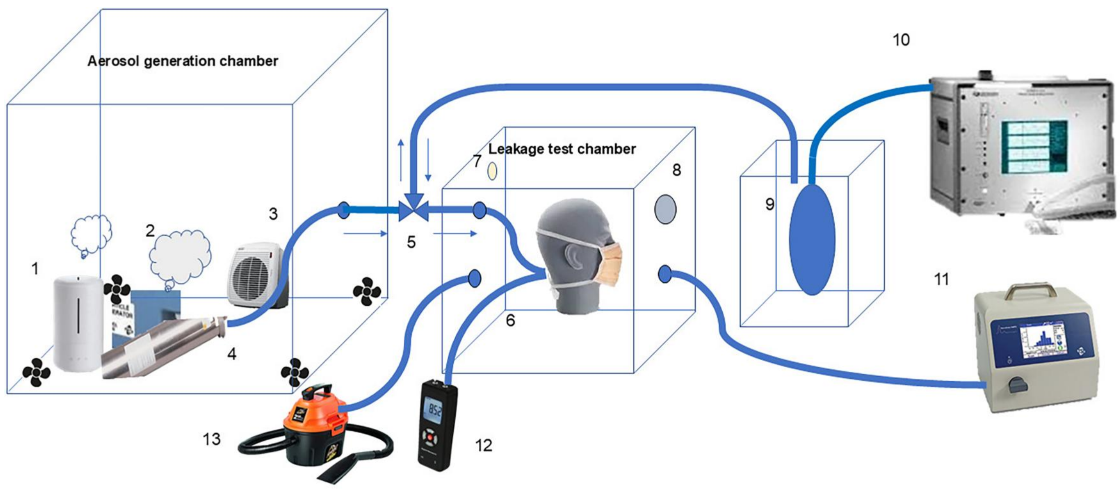

1. Humidifier; 2. Particle Generator; 3. Heater; 4. Neutralizer; 5. Three-way Valve; 6. Headform; 7. Inhalation Valve; 8. Exhalation Valve; 9. Bladder; 10. Breathing Simulator; 11. TSI NanoScan; 12. Pressure Monitor; 13. Vacuum

Figure 1. The schematic diagram of the test system (Myers et al. 2023).

measured the aerosol concentrations across different particle sizes upstream within the cavity formed between the headform and the device being tested. The concentrations of exhaled aerosols across different particle sizes downstream from the headform were quantified within the small chamber. We used a NanoScan SMPS (Model: 3910, TSI Inc., Shoreview, MN, USA) to measures nanoparticle size distributions from 0.01 to 0.42 µm. The challenge NaCl aerosol was generated by a TSI particle generator (Model 8026; TSI, Inc., Shoreview, MN, USA).

We kept the faceseal levels and flowrates in this study consistent with our previous study (Myers et al. 2023). The faceseal levels were determined by the percentage of the device's edge sealed on the headform using bees' wax. The 0% faceseal was achieved by simply mounting the device on the headform with no attempt to obtain any specific level of fit. The 50% faceseal was achieved by sealing one-half of the device to the headform. The 100% faceseal was achieved by completely sealing the device to the headform. The overall fit factors (FFs) of each device at these three faceseal levels are listed in Table 2. According to "ISO/TS 16976-1; Respiratory protective devices - Human factors - Part 1: Metabolic rates and respiratory flowrates" (International Organization for Standardization 2015), three flowrates of 17, 28, and 39 L/min were calculated to simulate the exhalation flowrate of healthcare workers with light, moderate, and heavy work rates, respectively. The body parameters used for the calculation were from studies by Zhu et al. (2019) and Williamson (2020), where the equations are shown in our previous study (Myers et al. 2023; Williamson 2020; Zhu et al. 2019).

The TOL for each device was based on the concentration downstream (outside of the device minus the background counts) divided by the concentration upstream (inside the device). We calculated the TOL_i for each particle size bin according to the equation in our companion study (Myers et al. 2023).

$$\text{TOL}_i = \frac{C_{ini} - C_{bgi}}{C_{outi}} \tag{1}$$

where

TOL_i = TOL of SM or half facepiece respirators for particles in group i having a midpoint size D_i

C_{ini} = Concentration inside the SM or half facepiece respirator cavity for particles in group i having a midpoint size D_i

C_{bgi} = Concentration of background in the leakage testing chamber for particles in group i having a midpoint size D_i

C_{outi} = Concentration outside SM or half mask respirator cavity in the leakage testing chamber for particles in group i having a midpoint size D_i

The midpoint size D_i was automatically calculated using the Multi-Instrument Manager (MIM®, version 3.0, TSI Inc., Shoreview, MN, USA) for each particle size interval. Additionally, we utilized a total of 9 particle size intervals in this study.

The most outward leakage particle size (MOLPS) corresponded to the particle size at which the TOL curve with particle sizes reached its peak value. We calculated the TOLMD and SD using Equations (2a) and (2b), respectively. The TOLMD was employed to measure the particle size characteristic of TOL.

Table 2. The overall FF of five devices at three different faceseal levels.

			Overall FF		
Device type	Manufacturer	Model	0% faceseal	50% faceseal	100% faceseal
EHMR	MSA	200LS	7	11	1097
	3M	7503	37	110	2592
EHMRSM	MSA, Cardinal Health	200LS	5	9	44,747
	3M, Cardinal Health	7503	32	67	5826
N95 FFR	3M	Aura9205	25	134	200+
	Fangtian	N058	2	4	200+
N95 FFRV	3M	Aura9211	9	71	200+
	3M	8511	4	13	200+
SM	Cardinal Health	–	3	4	137
	Aleen	–	5	5	193

$$\text{TOLMD} = \frac{\sum (D_i \times \ \text{TOL}_i)}{\sum \text{TOL}_i} \quad (2a)$$

$$SD = \frac{\sum((D_i\text{-TOLMD}) \times \text{TOL}_i)}{\sum \text{TOL}_i} \quad (2b)$$

where

D_i = midpoint particle size

TOL_i = TOL of particles in group i having a midpoint size D_i

This study encompassed 90 observations, including five device types, two replicates, three faceseal levels, and three flowrates. We calculated the TOLMD for each observation and conducted an ANOVA with a split-plot design using JMP Pro Software (JMP® version 16, SAS Institute Inc., Cary, NC, USA, 1989–2021) to evaluate the main effects of device type, faceseal level, flowrate; and the random effects of device model on TOLMD. p Values ≤ 0.05 were considered significant.

A linear statistical model for this split-plot design is (Montgomery 2017):

$$y_{ijkl} = \mu + \tau_i + \beta_j + (\tau\beta)_{ij} + \gamma_k + (\beta\gamma)_{jk} + \delta_l + (\beta\delta)_{jl} + (r\delta)_{kl} + (\beta\gamma\delta)_{jkl} + \epsilon_{ijkl} \begin{cases} i = 1, 2 \\ j = 1, 2, 3, 4, 5 \\ k = 1, 2, 3 \\ l = 1, 2, 3 \end{cases} \quad (3)$$

where τ_i is the error of replicates; $(\tau\beta)_{ij}$ is the whole plot error; β_j is the effect of device type; γ_k is the effect of faceseal; δ_l is the effect of flowrate; $(\beta\gamma)_{jk}$, $(\beta\delta)_{jl}$, $(r\delta)_{kl}$ and $(\beta\gamma\delta)_{jkl}$ are the interaction of these three factors, respectively; and ϵ_{ijkl} is the random error.

Results

Figure 2 displays the TOL_i values of five device types across particle sizes ranging from 20 to 210 nm at three faceseal levels. The TOL_i values in the graph were averaged across six observations (two replicates × three flowrates). The TOL of N95s FFR and SMs significantly varied with faceseal levels across particle sizes. When SMs were sealed at 0% and 50% on the headform, peak TOLs of 40% and 30%, respectively, were observed at the MOLPS of 90 nm. Upon improving the faceseal level to 100%, SMs exhibited a peak TOL of 20% at a MOLPS of 50 nm. N95 FFRs, with 0% and 50% faceseal, demonstrated the lowest TOLs of 13% and 6% at 40 nm, respectively, while N95 FFRs with 100% faceseal maintained the peak TOL at 40 nm. For particle sizes >40 nm, the TOL of N95 FFRs with 0% and 50% faceseal increased with particle size until reaching consistent TOL values of approximately 25% and 12%, respectively. This highlights that the 100% sealed N95 FFRs effectively mitigated TOL for particle sizes >40 nm.

The TOLs of the EHMR at three faceseal levels fluctuated with particle sizes ranging from 20 to 40 nm (Figure 2). However, they continued to increase when the particle size exceeded 40 nm, reaching TOLs around 90% for particle sizes around 210 nm. The EHMRSMs at three faceseal levels also exhibited a fluctuating trend in TOLs within the particle size range of 20–40 nm, eventually stabilizing at approximately 70%. The TOLs of N95 FFRVs at three faceseal levels decreased within the particle size range of 20–40 nm and increased within the particle size range of 40–90 nm. Subsequently, they stabilized at around 50% for both 0% and 50% faceseal levels and slightly decreased from 40% to 30% for the 100% faceseal level. The peak TOL value was observed at a MOLPS of 90 nm for N95 FFRVs at 100% faceseal.

Figure 3 displays the TOL_i values of five types of devices across particle sizes ranging from 20 to 210 nm at three flowrates. The TOL_i values in the figure represent mean values across six observations (two replicates ×three faceseal levels). The EHMRs, EHMRSMs, and N95 FFRVs exhibited a similar trend in TOL with particle size. It fluctuated in the particle size range of 20–40 nm, then increased and stabilized in the particle size range of 90–210 nm. These devices also demonstrated significant differences among

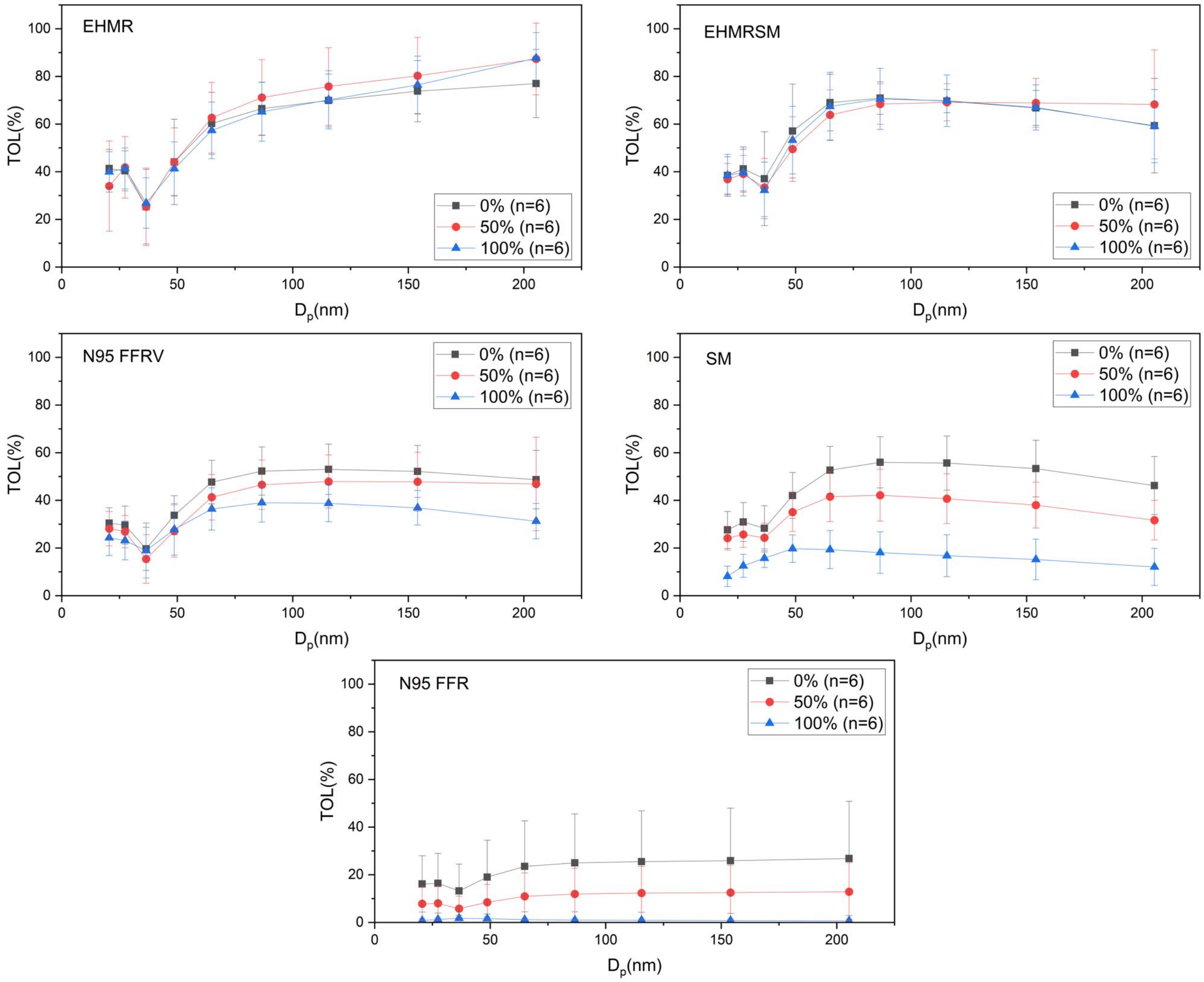

Figure 2. The TOL values of five types of devices as a function of particle size from 20 to 210 nm across faceseal levels.

flowrates in TOL across particle sizes. The EHMRs had TOLs that varied from ∼50% to ∼90% within the particle size range of 90–210 nm. The EHMRSMs showed TOLs varying from ∼50% to ∼80% within the particle size range of 90–210 nm. The N95 FFRVs exhibited TOLs varying from ∼30% to 50% within the particle size range of 90–210 nm.

The SMs and N95 FFRs did not show significant differences among flowrates in TOL across particle sizes (Figure 3). The SMs showed fluctuating TOLs across particle sizes from 20 to 40 nm, then increased to peak values of ∼35% to ∼40% around 90 nm and then slightly decreased. The N95 FFRs showed relatively consistent TOLs across particle sizes, which was around 10%.

The TOL mean diameter (TOLMD) and standard deviation (SD) values of each device type at different faceseal levels and flowrate combinations are listed in Table 3. The overall mean TOLMD for 90 observations in this study was 93 nm, with a SD of 11.7 nm. There is a range of TOLMD from 52 to 113 nm, varying with device type, faceseal, and flowrate.

The Analysis of Variance (ANOVA) results for TOLMD, categorized by device type, faceseal, flowrate, and their interactions, are presented in Table 4. The ANOVA indicates that device type (p value $= 0.0249$), faceseal (p value $= 0.0035$), and flowrate (p value $= 0.0199$) had significant effects on the TOLMD. The interaction of device type and faceseal (p value $= 0.034$) also demonstrated significant effects on the TOLMD.

Table 5 presents the mean TOLMD of each device type. The superscript letters behind the values indicate the statistically different levels according to the Student's t-test. The EHMRs, EHMRSMs, and N95 FFRVs had similar TOLMDs, ranging from 95 to 104 nm. The SMs and N95 FFRs had lower TOLMDs compared to the other devices, with values of 89 and 85 nm, respectively.

Table 6 lists the mean TOLMD values for all five device types at three faceseal levels. The Student's t-

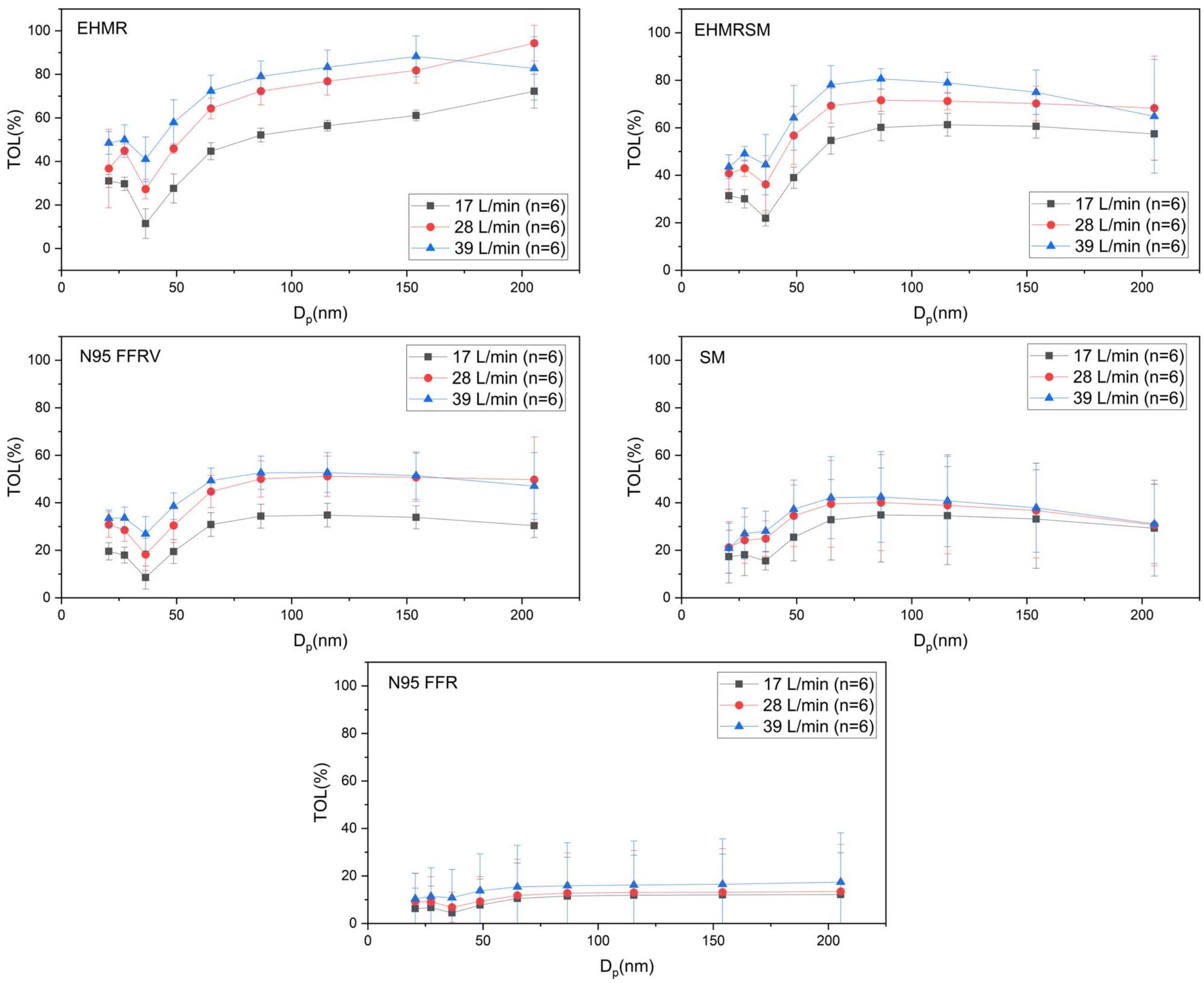

Figure 3. The TOL of five types of devices as a function of particle size ranging from 20 to 210 nm at three flowrates.

Table 3. The TOLMD and SD values of each device type at different faceseal level and flowrate combinations.

		TOLMD (nm) and SD at different faceseal and flowrate combinations								
		0% faceseal			50% faceseal			100% faceseal		
Device Type	Model	17 L/min	28 L/min	39 L/min	17 L/min	28 L/min	39 L/min	17 L/min	28 L/min	39 L/min
EHMR	3M 7503	111 (±63)	103 (±63)	106 (±64)	105 (±62)	111 (±59)	97 (±61)	104 (±62)	100 (±62)	104 (±65)
	MSA 200LS	102 (±61)	98 (±61)	93 (±59)	108 (±62)	105 (±63)	103 (±62)	113 (±64)	105 (±63)	102 (±62)
EHMRSM	3M 7503 & Cardinal Health	100 (±60)	100 (±62)	**	105 (±62)	101 (±63)	103 (±62)	98 (±60)	98 (±62)	95 (±59)
	MSA 200LS & Cardinal Health	98 (±58)	83 (±53)	84 (±53)	93 (±55)	93 (±57)	87 (±55)	98 (±58)	91 (±55)	85 (±53)
N95 FFRV	3M 8511	97 (±59)	95 (±59)	99 (±60)	102 (±60)	105 (±62)	90 (±57)	102 (±59)	94 (±58)	97 (±60)
	3 M 9211+	100 (±59)	95 (±57)	96 (±59)	94 (±57)	108 (±64)	95 (±57)	97 (±59)	89 (±56)	81 (±54)
SM	Aleen	99 (±59)	87 (±55)	93 (±57)	95 (±57)	90 (±57)	90 (±57)	88 (±55)	92 (±58)	86 (±55)
	Cardinal Health	100 (±59)	95 (±58)	90 (±57)	91 (±58)	87 (±57)	84 (±56)	78 (±52)	77 (±53)	74 (±50)
N95 FFR	FT N058	100 (±60)	98 (±61)	95 (±61)	101 (±61)	97 (±62)	94 (±61)	58 (±42)	52 (±32)	52 (±29)
	3 M 9205	95 (±61)	68 (±48)	96 (±62)	88 (±58)	110 (±61)	71 (±54)	99 (±65)	80 (±59)	79 (±59)

Note: **data was not valid and was deleted because of low upstream concentration.

test results indicate that the TOLMDs of 96 and 97 nm at 0% and 50% faceseal levels are comparable, while the TOLMD at 100% faceseal level is significantly lower, with a value of 89 nm.

In Table 7, the TOLMDs of each device type at different faceseal levels are listed. Statistical analysis using the Student's t-test revealed that the EHMRs, EHMRSMs, and N95 FFRVs did not demonstrate significant differences among the three faceseal levels within their respective types. Conversely, the SMs and N95 FFRs significantly reduced the TOLMD as the faceseal improved. Specifically, the TOLMDs of SMs decreased from 94 to 82 nm, and the TOLMDs of N95 FFRs decreased from 94 to 70 nm as faceseal

Table 4. The ANOVA results for TOLMD, categorized by device type, faceseal, flowrate, and their interactions.

Source	SS	MS	DF	F	*p* Value
Device type	3768.5	942.1	4	9.6361	0.0249*
Faceseal	1055.0	527.5	2	6.5611	0.0035*
Device type*Faceseal	1532.5	191.6	8	2.3827	0.034*
Flowrate	697.1	348.5	2	4.3351	0.0199*
Device type*Flowrate	52.1	6.5	8	0.0809	0.9996
Faceseal*Flowrate	425.4	106.3	4	1.3226	0.2786
Device type*Faceseal*Flowrate	554.6	34.7	16	0.4312	0.9638

Note: The *behind *p* values means there is a significant effect.

Table 5. The mean TOLMD of each device type with Student's t-test results.

Device type	Mean TOLMD (nm)	Std Dev	Lower 95%	Upper 95%
EHMR	103.9^{A}	5.1	97.4	110.4
N95 FFRV	96.4^{AB}	6.1	89.9	102.9
EHMRSM	94.8^{AB}	6.8	87.9	101.6
SM	88.7^{BC}	7.2	82.2	95.2
N95 FFR	85.2^{C}	17.9	78.8	91.7

Note: Levels not connected by same letter are significantly different.

Table 6. The mean TOLMD for all five device types at three faceseal levels with Student's t-test results.

Faceseal	Mean TOLMD (nm)	Std Dev	Lower 95%	Upper 95%
50%	96.8^{A}	9.1	93.5	100.1
0%	95.6^{A}	7.9	92.2	99.1
100%	89.0^{B}	15.2	85.7	92.3

Note: Levels not connected by same letter are significantly different.

improved from 0% to 100%. It is worth noting that the TOLMD of the N95 FFR was 70 nm, a value lower than that of the SM, which was 83 nm.

Table 8 presents the TOLMDs of SMs and half facepiece respirators at three flowrates. The results of the Student's t-test analysis revealed a significant decrease in TOLMD as flowrate increased, on average across all types of devices. Specifically, the mean TOLMD decreased from 97 nm at 17 L/min to 90 nm at 39 L/min.

Discussion

This study is the first to systematically measure the TOL of different respiratory protective devices and SMs specifically against submicron particles across a size range of 20–210 nm, offering a particle-size-specific analysis not addressed in previous research. Unlike our earlier work (Myers et al. 2023), which only evaluated overall TOL without distinguishing particle sizes, this study provides detailed insights into the probability of emission of submicron particles with varying diameters from source control devices. Additionally, the current investigation uniquely explores the effects of both faceseal integrity and flow rate on TOL in relation to particle size. These new findings build upon and significantly extend our

Table 7. The mean TOLMDs of each type of device at different faceseal levels with Student's t-test results.

Device type * Faceseal	Mean TOLMD (nm)	Std Dev	Lower 95%	Upper 95%
EHMR,50%	105.0^{A}	4.8	97.6	112.4
EHMR,100%	104.6^{AB}	4.2	97.2	112.0
EHMR,0%	102.2^{ABC}	6.4	94.8	109.6
N95 FFRV,50%	98.8^{ABCD}	7.2	91.4	106.3
N95 FFRV,0%	97.0^{ABCD}	2.1	89.6	104.4
EHMRSM,50%	96.9^{ABCD}	7.0	89.5	104.3
EHMRSM,100%	94.2^{BCD}	5.4	86.8	101.7
SM,0%	94.0^{CD}	4.9	86.6	101.4
N95 FFR,50%	93.7^{CD}	13.4	86.3	101.1
N95 FFRV,100%	93.3^{CD}	7.3	85.9	100.7
EHMRSM,0%	93.1^{CDE}	8.7	84.4	101.8
N95 FFR,0%	91.8^{CDE}	12.0	84.4	99.2
SM,50%	89.5^{DE}	3.7	82.1	96.9
SM,100%	82.6^{E}	7.1	75.1	90.0
N95 FFR,100%	70.2^{F}	19.0	62.8	77.6

Note: Levels not connected by same letter are significantly different.

Table 8. The TOLMDs of all five device types at three flowrates with Student's t-test results.

Flowrate (L/min)	Mean TOLMD (nm)	Std Dev	Lower 95%	Upper 95%
17	97.3^{A}	10.1	94.0	100.6
28	93.7^{AB}	12.6	90.4	97.0
39	90.4^{B}	11.4	87.0	93.8

Note: Levels not connected by same letter are significantly different.

previous research by providing a more comprehensive understanding of the efficacy of different source control devices.

The study underscored the crucial role of faceseal for both SMs and N95 FFRs in reducing TOL and minimizing particle size. As the faceseal of SMs and N95 FFRs improved, the TOL significantly decreased across particle sizes, especially for particles larger than 60 nm (Figure 2). Similar results for personal protection with SMs were found by Konda et al. (2020). The differences among the TOLMDs of SMs and N95 FFRs at three faceseal levels corroborated that the improved faceseal helps reduce the TOL for the larger particles.

When the N95 FFR and SM devices achieved a 100% seal to the headform, the TOL was solely attributed to particles penetrating through the filter during exhalation. A previous study suggested that the filtration efficiency of N95 FFRs notably surpasses that of SMs across various particle sizes (Zangmeister et al. 2020). In practice, N95 FFRs can achieve the 100% faceseal level if they have passed the fit test when worn by users, although this fit can vary based on individual facial characteristics (Spies, Wilson, and Ferrie 2011). On the other hand, SMs are typically loose-fitting and are not designed to achieve the same level of faceseal as N95 FFRs. Overall, SMs are inferior to N95 FFRs in terms of efficacy for source control.

The MOLPS of the N95 FFR with 100% faceseal devices falls within the MPPS range of 0.03–0.3 μm previously reported when the N95 FFR was used as protection for the wearer (Duncan, Bodurtha, and Naqvi 2021; Shaffer and Rengasamy 2009; Lee, Grinshpun, and Reponen 2008; Balazy et al. 2006; Qian et al. 1998). However, this study did not observe the MOLPS of N95 FFR with 0% and 50% faceseal levels. It is suggested that the MOLPS in these cases could be inferred to be greater than 210 nm, indicating the need for further research in this aspect with larger challenge aerosols.

It is noteworthy that TOL dropped around 35 nm when the N95 FFR and SM were not fully sealed on the headform, while no such drop occurred when these devices were 100% sealed. A similar pattern was observed in devices equipped with exhalation valves, including the N95 FFRV, EHMR, and EHMRSM. This phenomenon may be due to a combination of aerosol dynamics, surface interactions, and the design of the respiratory devices, particularly in the presence of leakage pathways, such as faceseal gaps or exhalation valves (Harley and Ruzer 1998; Dahneke 1971). One plausible explanation is that aerosols emitted through faceseal gaps may interact with the headform surface, allowing smaller particles to be captured *via* Brownian motion. Likewise, in devices with exhalation valves, particles could interact with the surface within respirator cavity and flap of the valve, leading to capture or deflection within the valve. This would result in a reduction in outward leakage for aerosols within this specific particle size range. However, the precise mechanisms behind particle capture through faceseal gaps and exhalation valves warrant further investigation.

The findings of this study suggest that EHMRs (with unfiltered exhalation valves) may not be effective in containing the emission of submicron particles, particularly those larger than 100 nm. The TOLs of EHMRs exhibited an increasing trend as the particle size increased from 40 to 210 nm, reaching approximately 90%. This trend indicated a high likelihood of emitting larger submicron particles when EHMRs are used for source control. This can be attributed to the presence of an exhalation valve in the latter devices. The valve permits a substantial release of submicron particles through exhalation rather than filtration filters. However, it is essential to note that Brownian diffusion remains the most effective method for capturing particles $<$200 nm (Tcharkhtchi et al. 2021).

It is worth noting that SARS-CoV-2 virions have been found to be carried in particles ranging from approximately 0.1 to 10 μm (Pöhlker et al. 2021). While the study examined aerosols in the range of 20–210 nm, which are less likely to carry viruses, they exhibit high concentrations when exhaled by humans, thereby posing a risk for the spread of viruses (Bagheri et al. 2023). Thus, the inability to block the emission of submicron particles $>$100 nm by EHMRs used for source control raises concerns about their adequacy in preventing the spread of respiratory diseases, including COVID-19.

Despite the presence of an SM covering the exhalation valve, EHMRSMs did not show a significant improvement in reducing the TOL for submicron particles $>$100 nm. To enhance source control, the use of non-valved EHMRs or EHMRs with filters on the exhalation valve have been devloped and got NIOSH Approved (CDC 2023). These improved EHMRs can both filter the particles inward and outward during breathing. Although NIOSH approval for elastomeric half-mask respirators (EHMRs) with filters or non-valved options is an important step toward ensuring source control, the efficacy of these alternative devices in terms of source control still needs to be evaluated.

The decrease in TOLMDs with increasing flowrate revealed an increase in TOL for smaller submicron particles. It may be because the higher airflow velocity weakened the effects of Brownian diffusion, which caused more penetration of smaller submicron particles through filters (Adanur and Jayswal 2022; Tcharkhtchi et al. 2021). The differences among the TOLMDs of SMs and N95 FFRs at three faceseal levels corroborated that the improved faceseal helps reduce the TOL and minimize the size of particle within the leakage.

Even though the submicron particles ranging from 20 to 210 nm do not carry a large amount of viruses, it should be noted that these submicron particles make up a large portion of exhaled aerosols and can suspend in the ambient environment for a long time (Bagheri et al. 2023). The 1 μm aerosols could remain suspended in the air for more than 12 h (Wang et al. 2021). Aerosols $\sim$100 nm in size could even suspend in the air over multiple days (Lee 2020). In this case, dilution ventilation is crucial in indoor environments, especially healthcare settings, to prevent inhalable infectious aerosols from accumulating in the room, especially if improper or poor-fitted face masks and half facepiece respirators are being used for source control.

This study has several limitations. One major limitation is that the particle sizes generated by our laboratory system were relatively small, and did not fully replicate the range of particle sizes produced by human respiration, particularly the larger micron-sized particles, which may carry a higher viral load.

Although both the TSI NanoScan and Optical Particle Sizer (OPS) were initially employed to collect aerosol concentration data, the concentration inside the mask or respirator detected by the OPS was extremely low. This introduced uncertainty in the TOL measurements at specific particle sizes. As a result, this study focused primarily on the particle size data collected by the TSI NanoScan, which yielded more reliable results. Further studies are needed to examine TOL across a broader range of larger particle sizes. Additionally, another limitation stems from the relatively small sample size for devices within each type. Testing a broader range of models is essential to obtain a more representative reflection of the performance of existing source control devices. Moreover, this study did not simulate respiratory activities such as coughing and sneezing that pose more significant challenges to source control. It is imperative to assess the efficacy of source control devices in mitigating particles emitted during these respiratory activities across different particle sizes.

Conclusions

This study investigated the TOL of five types of source control devices against submicron particles in the function of particle size ranging from 20 to 210 nm, offering a more granular analysis than our previous research. In contrast to earlier work, which focused solely on overall TOL, this study provides a detailed exploration of how faceseal quality and flowrate influence TOL across different particle sizes. The findings underscored a significant concern regarding the efficacy of EHMRs and EHMRSMs. Given that SARS-CoV-2 viruses are likely to be carried in aerosols ranging from 0.1 to 10 μm (Pöhlker et al. 2021), the high TOL of EHMRs and EHMRSMs for submicron particles with diameters $>$100 nm raised substantial doubts about their efficacy as source control.

These findings underscore the crucial role that the faceseal has in reducing the TOL of larger submicron particles potentially carrying viruses for SMs and N95 FFRs. Fit testing is essential for N95 FFRs because an inadequate faceseal compromises their efficacy in reducing the spread of exhaled aerosols. Measures to improve the faceseal of SMs need to be explored.

Overall, caution is warranted when selecting respiratory protective devices with exhalation valves for source control due to their potentially high TOL for submicron particles based on this study's findings. Well-fitting N95 FFRs are likely to improve source control. Future studies should investigate the TOL of these source control devices across a broader range of particle sizes, particularly larger micron-sized particles that may carry more viruses.

Nomenclature

TOL	total outward leakage
TOLMD	total outward leakage mean diameter
SD	standard deviation
N95 FFR	N95 filtering facepiece respirators
N95 FFRV	N95 filtering facepiece respirators with an exhalation valve
SM	surgical mask
EHMR	elastomeric half mask respirator
EHMRSM	elastomeric half mask respirator with a surgical mask covering the exhalation valve
NIOSH	National Institute for Occupational Safety and Health
MPPS	most penetrating particle size
MOLPS	most outward leakage particle size

Acknowledgment

The authors would like to thank National Personal Protective Technology Laboratory staff members William Lindsley, Lee Greenawald, Kevin Strickland, and other NIOSH members for their review of this article. N95 and NIOSH Approved are certification marks of the U.S. Department of Health and Human Services (HHS) registered in the United States and several international jurisdictions.

Author contributions statement and ethics

W.Y., W.R.M., and Z.Z. contributed to the conception and design of the work. W.Y. was responsible for the data collection. W.Y, W.R.M., K.J.R., L.P., M.B., E.F., B.V., and Z.Z. performed data analyses and drafted the manuscript. W.Y., K.J.R., and W.R.M contributed to the statistical analyses. All authors reviewed and gave critical comments on the manuscript. All authors revised the manuscript and approved the final version to be submitted.

Disclosure statement

No potential conflict of interest was reported by the author(s).

Disclaimer

The findings and conclusions in this report are those of the authors and do not necessarily represent the official position of the National Institute for Occupational Safety and Health, Centers for Disease Control and Prevention. Mention of any company or product does not constitute endorsement by the National Institute for Occupational Safety and Health, Centers for Disease Control and Prevention.

Declaration of interest statement

The authors declare no competing interests.

Funding

This study was funded by the National Institute for Occupational Safety and Health (NIOSH), National Personal Protective Technology Laboratory (NPPTL) (Contract # 75D30120P09521).

ORCID

Weihua Yang http://orcid.org/0000-0002-2849-2786
Mike Bergman http://orcid.org/0000-0002-2742-6197
Lee Portnoff http://orcid.org/0000-0002-3768-9361

Data availability statement

The data will be available on the NIOSH Data and Statistics Gateway once cleared by NIOSH.

References

Adanur, S., and A. Jayswal. 2022. Filtration mechanisms and manufacturing methods of face masks: An overview. *J. Ind. Text.* 51 (3):3683S–717S. doi: 10.1177/1528083720980169.

ASTM. 2020. *Specification for Performance of Materials Used in Medical Face Masks. West* Conshohocken, PA: ASTM.

Bagheri, G., O. Schlenczek, L. Turco, B. Thiede, K. Stieger, J. M. Kosub, S. Clauberg, M. L. Pöhlker, C. Pöhlker, J. Moláček, et al. 2023. Size, concentration, and origin of human exhaled particles and their dependence on human factors with implications on infection transmission. *J. Aerosol. Sci.* 168:106102. doi: 10.1016/j.jaerosci.2022.106102.

Balazy, A., M. Toivola, T. Reponen, A. Podgórski, A. Zimmer, and S. A. Grinshpun. 2006. Manikin-based performance evaluation of N95 filtering-facepiece respirators challenged with nanoparticles. *Ann. Occup. Hyg.* 50 (3): 259–69. doi: 10.1093/annhyg/mei058.

Bourouiba, L. 2021. The fluid dynamics of disease transmission. *Annu. Rev. Fluid Mech.* 53 (1):473–508. doi: 10.1146/annurev-fluid-060220-113712.

CDC. 2023. CDC-NIOSH-NPPTL: Certified equipment list search results. Accessed May 14, 2023. https://wwwn.cdc.gov/NIOSH-CEL/Results?Schedule=84A&FacepieceType=Half+Mask&Valveless=true&Precision=inclusive&contaminants=32&contaminants=33&contaminants=34&contaminants=35&contaminants=36&contaminants=37&contaminants=38&contaminants=39&contaminants=40

CDC. 2022. Healthcare workerscent. Dis. Control Prev. Accessed August 17, 2022. https://www.cdc.gov/coronavirus/2019-ncov/hcp/infection-control-recommendations.html

Chatterjee, S., J. S. Murallidharan, A. Agrawal, and R. Bhardwaj. 2021. How coronavirus survives for hours in aerosols. *Phys. Fluids (1994)* 33 (8):081708. doi: 10.1063/5.0059908.

Cheng, Y., N. Ma, C. Witt, S. Rapp, P. S. Wild, M. O. Andreae, U. Pöschl, and H. Su. 2021. Face masks effectively limit the probability of SARS-CoV-2 transmission. *Science* 372 (6549):1439–43. doi: 10.1126/science.abg6296.

Dahneke, B. 1971. The capture of aerosol particles by surfaces. *J. Colloid Interface Sci.* 37 (2):342–53. doi: 10.1016/0021-9797(71)90302-X.

Duncan, S., P. Bodurtha, and S. Naqvi. 2021. The protective performance of reusable cloth face masks, disposable procedure masks, KN95 masks and N95 respirators: Filtration and total inward leakage. *PLoS One.* 16 (10): e0258191. doi: 10.1371/journal.pone.0258191.

Fennelly, K. P. 2020. Particle sizes of infectious aerosols: Implications for infection control. *Lancet. Respir. Med.* 8 (9):914–24. doi: 10.1016/S2213-2600(20)30323-4.

Grinshpun, S. A., and M. Yermakov. 2021. Technical note: Impact of face covering on aerosol transport patterns during coughing and sneezing. *J. Aerosol Sci.* 158:105847. doi: 10.1016/j.jaerosci.2021.105847.

Harley, N. H., and L. S. Ruzer. 1998. *Aerosols Handbook.* Boca Raton, FL: CRC Press.

International Organization for Standardization. 2015. *Respiratory Protective Devices - Human Factors - Part 1: Metabolic Rates and Respiratory Flow Rates.* Geneva, Switzerland: International Organization for Standardization.

Joshi, M., A. Khan, and B. Sapra. 2022. Quick laboratory methodology for determining the particle filtration efficiency of face masks/respirators in the wake of COVID-19 pandemic. *J. Ind. Text.* 51 (5):7622S–40S. doi: 10.1177/1528083720975084.

Konda, A., A. Prakash, G. A. Moss, M. Schmoldt, G. D. Grant, and S. Guha. 2020. Aerosol filtration efficiency of common fabrics used in respiratory cloth masks. *ACS Nano.* 14 (5):6339–47. doi: 10.1021/acsnano.0c03252.

Lee, B. U. 2020. Minimum sizes of respiratory particles carrying SARS-CoV-2 and the possibility of aerosol generation. *Int. J. Environ. Res. Public Health.* 17 (19):6960. doi: 10.3390/ijerph17196960.

Lee, S. A., S. A. Grinshpun, and T. Reponen. 2008. Respiratory performance offered by N95 respirators and surgical masks: Human subject evaluation with NaCl aerosol representing bacterial and viral particle size range. *Ann. Occup. Hyg.* 52 (3):177–85. doi: 10.1093/annhyg/men005.

Lindsley, W. G., F. M. Blachere, D. H. Beezhold, B. F. Law, R. C. Derk, J. M. Hettick, K. Woodfork, W. T. Goldsmith, J. R. Harris, M. G. Duling, et al. 2021a. A comparison of performance metrics for cloth masks as source control devices for simulated cough and exhalation aerosols. *Aerosol. Sci. Technol.* 55 (10):1125–42. doi: 10.1080/02786826.2021.1933377.

Lindsley, W. G., F. M. Blachere, B. F. Law, D. H. Beezhold, and J. D. Noti. 2021b. Efficacy of face masks, neck gaiters and face shields for reducing the expulsion of simulated cough-generated aerosols. *Aerosol. Sci. Technol.* 55 (4): 449–57. doi: 10.1080/02786826.2020.1862409.

Lu, H., D. Yao, J. Yip, C.-W. Kan, and H. Guo. 2020. Addressing COVID-19 Spread: Development of Reliable Testing System for Mask Reuse. *Aerosol. Air Qual. Res.* 20 (11):2309–17. doi: 10.4209/aaqr.2020.06.0275.

Milton, D. K., M. P. Fabian, B. J. Cowling, M. L. Grantham, and J. J. McDevitt. 2013. Influenza birus aerosols in human exhaled breath: Particle size, culturability, and effect of surgical masks. *PLoS Pathog.* 9 (3):e1003205. doi: 10.1371/journal.ppat.1003205.

Mittal, R., R. Ni, and J. H. Seo. 2020. The flow physics of COVID-19. *J. Fluid Mech.* 894:F2. doi: 10.1017/jfm.2020.330.

Montgomery, D. C. 2017. *Design and Analysis of Experiments*. Hoboken, NJ: John Wiley & Sons.

Myers, W., S. Ajewole, S. Xu, P. Yorio, A. Hornbeck, and Z. Zhuang. 2022. Laboratory assessment of bacterial contamination of a sterile environment when using respirators not traditionally used in a sterile field environment. *Infect. Control Hosp. Epidemiol.* 43 (12):1867–72. doi: 10.1017/ice.2022.122.

Myers, W. R., W. Yang, K. J. Ryan M. S. Bergman, E. M. Fisher, J.-C Soo, and Z. Zhuang 2023. Total outward leakage of half-mask respirators and surgical masks used for source control. *J. Occup. Environ. Hyg.* 20 (12):610–20. doi: 10.1080/15459624.2023.2257254.

Pöhlker, M. L., O. O. Krüger, J.-D. Förster, T. Berkemeier, W. Elbert, J. Fröhlich-Nowoisky, U. Pöschl, C. Pöhlker, G. Bagheri, E. Bodenschatz, et al. 2021. Respiratory aerosols and droplets in the transmission of infectious diseases. *Rev. Mod. Phys.* 95 (4):045001. doi: 10.1103/RevModPhys.95.045001.

Portnoff, L., J. Schall, J. Brannen, N. Suhon, K. Strickland, and J. Meyers. 2021. Filtering facepiece respirators with an exhalation valve: Measurements of filtration efficiency to evaluate their potential for source control. By U.S. Department of Health and Human Services, Centers for Disease Control and Prevention, National Institute for Occupational Safety and Health, DHHS (NIOSH) Publication No. 2021-107. doi: 10.26616/NIOSHPUB2021107.

Prather, K. A., L. C. Marr, R. T. Schooley, M. A. McDiarmid, M. E. Wilson, and D. K. Milton. 2020. Airborne transmission of SARS-CoV-2. *Science* 370 (6514):303–4. doi: 10.1126/science.abf0521.

Prather, K. A., C. C. Wang, and R. T. Schooley. 2020. Reducing transmission of SARS-CoV-2. *Science* 368 (6498):1422–4. doi: 10.1126/science.abc6197.

Qian, Y., K. Willeke, S. A. Grinshpun, J. Donnelly, and C. C. Coffey. 1998. Performance of N95 respirators: Filtration efficiency for airborne microbial and inert particles. *Am. Ind. Hyg. Assoc. J.* 59 (2):128–32. doi: 10.1080/15428119891010389.

Rengasamy, S., B. Eimer, and R. E. Shaffer. 2010. Simple respiratory protection—evaluation of the filtration performance of cloth masks and common fabric materials against 20–1000 nm size particles. *Ann. Occup. Hyg.* 54 (7):789–98. doi: 10.1093/annhyg/meq044.

Samet, J. M., K. Prather, G. Benjamin, S. Lakdawala, J. M. Lowe, A. Reingold, J. Volckens, and L. C. Marr. 2021. Airborne transmission of severe acute respiratory syndrome coronavirus 2 (SARS-CoV-2): What we know. *Clin. Infect. Dis.* 73 (10):1924–6. doi: 10.1093/cid/ciab039.

Shaffer, R. E., and S. Rengasamy. 2009. Respiratory protection against airborne nanoparticles: A review. *J. Nanopart. Res.* 11 (7):1661–72. doi: 10.1007/s11051-009-9649-3.

Spies, A., K. S. Wilson, and R. Ferrie. 2011. Respirator fit of a medium mask on a group of South Africans: A cross-sectional study. *Environ. Health.* 10 (1):17. doi: 10.1186/1476-069X-10-17.

Staymates, M. 2020. Flow visualization of an N95 respirator with and without an exhalation valve using schlieren imaging and light scattering. *Phys. Fluids (1994)* 32 (11):111703. doi: 10.1063/5.0031996.

Tcharkhtchi, A., N. Abbasnezhad, M. Zarbini Seydani, N. Zirak, S. Farzaneh, and M. Shirinbayan. 2021. An overview of filtration efficiency through the masks: Mechanisms of the aerosols penetration. *Bioact. Mater.* 6 (1):106–22. doi: 10.1016/j.bioactmat.2020.08.002.

Verma, S., M. Dhanak, and J. Frankenfield. 2020. Visualizing droplet dispersal for face shields and masks with exhalation valves. *Phys. Fluids (1994)* 32 (9):091701. doi: 10.1063/5.0022968.

Wang, C. C., K. A. Prather, J. Sznitman, J. L. Jimenez, S. S. Lakdawala, Z. Tufekci, and L. C. Marr. 2021. Airborne transmission of respiratory viruses. *Science* 373 (6558):eabd9149. doi: 10.1126/science.abd9149.

Williamson, S. R. 2020. *Respiratory Flow Characteristics of Intensive Care Healthcare Workers Performing Patient Care Activities* (M.S.). Morgantown, WV: West Virginia University.

World Health Organization. 2024. *Global Technical Consultation Report on Proposed Terminology for Pathogens that Transmit through the Air*. Geneva, Switzerland: World Health Orgnization.

Zangmeister, C. D., J. G. Radney, E. P. Vicenzi, and J. L. Weaver. 2020. Filtration efficiencies of nanoscale aerosol by cloth mask materials used to slow the spread of SARS-CoV-2. *ACS Nano.* 14 (7):9188–200. doi: 10.1021/acsnano.0c05025.

Zhu, J., X. He, M. S. Bergman, S. Guffey, A. D. Nimbarte, and Z. Zhuang. 2019. A pilot study of minimum operational flow for loose-fitting powered air-purifying respirators used in healthcare cleaning services. *J. Occup. Environ. Hyg.* 16 (7):440–5. doi: 10.1080/15459624.2019.1605241.